

Atomic spectroscopy with twisted photons: Separation of $M1$ - $E2$ mixed multipolesAndrei Afanasev,¹ Carl E. Carlson,² and Maria Solyanik¹¹*Department of Physics, The George Washington University, Washington, D.C. 20052, USA*²*Department of Physics, The College of William and Mary in Virginia, Williamsburg, Virginia 23187, USA*

(Received 9 January 2018; published 26 February 2018)

We analyze atomic photoexcitation into the discrete states by twisted photons, or photons carrying extra orbital angular momentum along their direction of propagation. From the angular momentum and parity considerations, we are able to relate twisted-photon photoexcitation amplitudes to their plane-wave analogs, independently of the details of the atomic wave functions. We analyze the photoabsorption cross sections of mixed-multipolarity $E2$ - $M1$ transitions in ionized atoms and found fundamental differences coming from the photon topology. Our theoretical analysis demonstrates that it is possible to extract the relative transition rates of different multipolar contributions by measuring the photoexcitation rate as a function of the atom's position (or impact parameter) with respect to the optical vortex center. The proposed technique for separation of multipoles can be implemented if the target's atom position is resolved with subwavelength accuracy; for example, with Paul traps. Numerical examples are presented for Boron-like highly charged ions.

DOI: [10.1103/PhysRevA.97.023422](https://doi.org/10.1103/PhysRevA.97.023422)

I. INTRODUCTION

Twisted photons, or topological states of light, carrying extra orbital angular momentum (OAM) along their propagation direction, have been one of the trends in optics, photonics, and related studies of light-matter interaction for more than 20 years. The seminal paper by Allen *et al.* [1] triggered major development in the field of optical control and manipulation, microscopy, telecommunication, information security, etc. In atomic photoexcitation by twisted photons, the terms responsible for vortex behavior can often be conveniently factorized from the conventional plane-wave contribution [2]. Modified atomic selection rules were worked out for Bessel beams (BBs) [2–4]. Later, the formalism was extended to Laguerre–Gaussian (LG) beams [5]. The fact that total angular momentum of twisted photons can be passed to the internal degrees of freedom of an atom was confirmed experimentally for quadrupole transitions with trapped ions [6,7] and agreed with theoretical predictions. Atomic photoexcitation by vortex beams as a local probe of the beam's topological structure was discussed in Ref. [8]. A physics argument for varied strengths for different multipole transitions across the twisted-light wavefront can be found in Ref. [9]: While dipole transitions are driven by the electromagnetic field intensity, the quadrupole transitions are caused by the field gradients. For a recent review of interactions between the twisted photons and atoms, see Ref. [10].

The phenomena for the trapped ions interacting with twisted photons have potential applications in quantum computing and quantum storage [11,12] due to extra photon-OAM degrees of freedom. Long lifetimes of forbidden states and abundance of nearly degenerate transitions are important benefits for optical-clock candidates [13]. Since even a moderate, 3%–5%, increase in lifetime is important, twisted light can be used as a tool for local high-precision control and tuning of the transition

rates. It would allow development of temporal, as well as spatial, measurement techniques based on the knowledge of transition rates with high multipolarity.

Dipole-forbidden transitions are important for measurements of uncertainties in atomic structure and for probing physics beyond the standard model [14] as well as astrophysics [15], and many other related fields; see Ref. [16] for review. Transitions forbidden by $E1$ selection rules recently received a lot of attention in precision spectroscopy [17–20]. In this respect, we are particularly interested in studying an interplay of topological properties of the incoming radiation and the atomic system.

The content of the transitions with mixed multipolarity can be extracted from independent measurements of the transition rates excited by the photons of opposite helicity. Search and tabulation of atomic transitions with mixed multipolarity goes back to the 1920s. The technique of using the Zeeman effect to separate different multipolar contributions in such processes is laid out in Ref. [21]. The particular transitions with $M1$ - $E2$ multipolarity in Bi I, and Pb I and II were studied extensively in Refs. [22–24], where separation of multipolar contributions was analyzed both theoretically and experimentally. The techniques for numerical analysis with extraction of the hyperfine structure for the cases of both integer and half-integer spin were discussed, for instance, in Ref. [25].

A theoretical description of the photon-atom interaction in a total-angular-momentum (TAM) basis is the main focus of this paper. The convenient separation of the TAM into orbital and spin parts violates gauge invariance [26], which motivates us to work in the TAM basis instead of the conventional linear momentum representation. In the Sec. II we briefly review the quantum-mechanical formalism of photoabsorption of the BB and Bessel–Gauss (BG) light beams by atoms. Section III is dedicated to revisiting the QED description of the photon vector potential in the TAM basis. In Sec. IV we use this

formalism to derive the photoabsorption amplitude in terms of spherical multipoles for the case of twisted light and discuss the distinct features in the photoabsorption cross section of ions caused by the topology of the incoming beam and OAM transfer to the atomic degrees of freedom. In Sec. V the results are summarized.

II. ABSORPTION OF TWISTED PHOTONS BY ATOMS

In this section we consider two modes of twisted-light beams: BB and BG. Even though all of them represent optical beam-like fields, they belong to fundamentally different families. BB is an example of nonparaxial mode, structurally stable under propagation. BG is the Helmholtz-type beam which satisfies the paraxial wave equation and is characterized by BB-like behavior close to the beam axis and Gaussian-like decay on the periphery.

The fundamental difference between the nonparaxial BB, and paraxial BG modes is that the former one satisfies Maxwell's equations, while the latter ones, strictly speaking, do not. However, one can still apply conventional QED methods to BG modes for the case of not-tightly focused paraxial beams.

Photoexcitation by BB is the convenient place to start due to the elegance of mathematical representation and the property of Bessel functions to form a complete orthonormal basis. These allow us to simply expand the other beam-like solutions in terms of Bessel modes with further application of the developed formalism.

A. Bessel mode

As is well known (see, e.g., Ref. [27]), when solving the scalar Helmholtz equation in cylindrical coordinates (ρ, ϕ, z) , one obtains Bessel modes

$$u^{(\text{BB})}(\rho, \phi, z; t) = A J_{m_\gamma}(\kappa \rho) e^{i(m_\gamma \phi - k_z z)} e^{i\omega t} + \text{c.c.}, \quad (1)$$

where m_γ is the projection twisted photon's TAM on the direction of propagation; $J_{m_\gamma}(x)$ is the Bessel function of the first kind, and k_z and κ are respectively longitudinal and transverse components of the photon's wave vector with respect to the propagation direction z . The normalization constant $A = \sqrt{\kappa/2\pi}$. Following the conventional quantization procedure requires the plane-wave expansion of the mode. We use the angular spectrum representation (see, e.g., Ref. [28]), so that the vector solution can be written as

$$\begin{aligned} \hat{A}_{k_z \kappa m_\gamma \Lambda}(\mathbf{r}, t) &= A \sqrt{\frac{2\pi}{\omega}} \sum_k \sum_{\Lambda=-1,1} \int \frac{d^2 k_\perp}{(2\pi)^2} a_{\kappa m_\gamma} \\ &\times \{ \hat{a}_{k\Lambda} \mathbf{e}_{k\Lambda} e^{i(\mathbf{k} \cdot \mathbf{r} - \omega t)} + \hat{a}_{k\Lambda}^\dagger \mathbf{e}_{k\Lambda}^\dagger e^{-i(\mathbf{k} \cdot \mathbf{r} - \omega t)} \}. \end{aligned} \quad (2)$$

Here $a_{\kappa m_\gamma}$ is the component of the two-dimensional (2D) Fourier transform [2,29]; $\Lambda = \pm 1$ is (spin) helicity of the plane-wave photons forming the Bessel mode, and $\mathbf{e}_{k\Lambda}$ is the basis state of the twisted-photon polarization, which relates to the plane photon polarization vectors by an SO(3) rotation group transformation $\hat{R}_z(-\phi_k) \hat{R}_y(-\theta_k)$ to the linear polariza-

tion basis [30,31]:

$$\mathbf{e}_{k\Lambda} = e^{-i\Lambda\phi_k} \cos^2 \frac{\theta_k}{2} \eta_\Lambda^\mu + e^{i\Lambda\phi_k} \sin^2 \frac{\theta_k}{2} \eta_{-\Lambda}^\mu + \frac{\Lambda}{\sqrt{2}} \sin \theta_k \eta_0^\mu, \quad (3)$$

where θ_k is commonly called a pitch angle and ϕ_k is the azimuthal angle [2]. Note that $\Lambda = 1$ (-1) corresponds to right-circular (left-circular) polarization (RCP and LCP, respectively). The corresponding local (e.g., at atom's center) photon flux is

$$\begin{aligned} f(\mathbf{b}) &= \cos(\theta_k) (|E|^2 + |B|^2)/4 \\ &= \cos(\theta_k) \frac{A^2 \omega^2}{2} \left\{ \cos^4 \frac{\theta_k}{2} J_{m_\gamma - \Lambda}^2(\kappa b) \right. \\ &\quad \left. + \sin^4 \frac{\theta_k}{2} J_{m_\gamma + \Lambda}^2(\kappa b) + \frac{\sin^2 \theta_k}{2} J_{m_\gamma}^2(\kappa b) \right\}, \end{aligned} \quad (4)$$

where \mathbf{b} is an *impact parameter*, or the atom's transverse location with respect to the optical vortex axis. Note that the use of impact-parameter representation for the absorption of twisted light by atoms was demonstrated to be especially practical in Ref. [32].

Proceeding with this approach, the convenient factorization property of the twisted photo-absorption amplitude was obtained [2–4]:

$$\begin{aligned} |M_{m_f, m_i}^{(\text{BB})}(b)| &= \frac{A}{2\pi} \left| J_{m_f - m_i - m_\gamma}(\kappa b) \sum_{m'_f, m'_i} d_{m'_f, m'_i}^{j_f} \right. \\ &\quad \left. \times (\theta_k) d_{m_i, m'_i}^{j_i}(\theta_k) M_{m'_f, m'_i}^{(\text{pw})}(\theta_k = 0) \right|, \end{aligned} \quad (5)$$

where $j_{i(f)}$ and $m_{i(f)}$ are TAM of initial (and final) atomic levels and their projections, respectively. The two terms responsible for the modification of the selection rules are Wigner d functions and Bessel function of the first kind $J_{m_f - m_i - m_\gamma}(\kappa b)$, which in the limiting case of a small impact parameter $b \rightarrow 0$ results in the constraint specific for the twisted light: $m_\gamma = m_f - m_i$. It implies that at the center of the optical vortex, the TAM projection m_γ of the incoming photon precisely matches the difference in magnetic quantum numbers of initial and final Zeeman levels, while other transitions are forced to zero by angular-momentum conservation. This behavior of twisted-light absorption was demonstrated experimentally with $^{40}\text{Ca}^+$ ions in a Paul trap [6,7].

B. Bessel-Gauss mode

The BG mode, first discussed in Ref. [33], is known to be a reliable mathematical representation of real photon laser modes both on the periphery and at the central region. It satisfies the paraxial equation [34] and carries a well-defined TAM:

$$u^{(\text{BG})}(\rho, \phi, z; t) = A J_{m_\gamma}(\kappa \rho) e^{-\rho^2/w_0^2} e^{im_\gamma \phi} e^{-i(k_z z - \omega t)} + \text{c.c.} \quad (6)$$

Making use of the angular spectrum representation, the corresponding photoexcitation amplitude can be expressed as

$$|M_{m_f, m_i}^{(\text{BG})}(b)| = e^{-b^2/\omega_0^2} \frac{A}{2\pi} \left| J_{m_f - m_i - m_y}(\kappa b) \sum_{m'_f, m'_i} d_{m'_f, m'_i}^{j_f} \times (\theta_k) d_{m_i, m'_i}^{j_i}(\theta_k) M_{m'_f, m'_i}^{(\text{pw})}(\theta_k = 0) \right|, \quad (7)$$

For details of these derivations we refer the reader to the recent paper by Afanasev *et al.* [7].

III. EXPANSION IN SPHERICAL HARMONICS

As was argued in Ref. [35], quantum states of nonparaxial beams, such as BB, are not well defined in the linear momentum basis. Instead, the photon's TAM (j) basis is used, with minimum $6 \leq 2(2j+1)$ possible states. The vector potential in terms of spherical multipoles can be defined as

$$\mathbf{A}_{jm}^M(k, \mathbf{r}) = j_j(kr) \mathbf{Y}_{jm}(\Omega), \quad (8)$$

$$\mathbf{A}_{jm}^E(k, \mathbf{r}) = \left(\sqrt{\frac{j+1}{2j+1}} j_{j-1}(kr) \mathbf{Y}_{j, j-1, m}(\Omega) - \sqrt{\frac{j}{2j+1}} j_{j+1}(kr) \mathbf{Y}_{j, j+1, m}(\Omega) \right), \quad (9)$$

where M and E stand for vector fields of the magnetic and electric type, correspondingly; $j_m(x)$ is the spherical Bessel function; and $\mathbf{Y}_{j, \ell, m}(\Omega)$ are vector spherical harmonics (see, e.g., Refs. [36]).

In the Coulomb gauge, the nonrelativistic quantum-mechanical photoabsorption matrix element can be written as

$$S_{fi} = -i \int dt \langle n_f j_f m_f | H_{\text{int}} | n_i j_i m_i; k \Lambda \rangle, \quad (10)$$

where the Hamiltonian operator H_{int} includes both charge- and spin-dependent parts. For the incoming plane-wave state with well-defined (LCP or RCP) helicity, the corresponding matrix element is

$$M_{m_f m_i}^{(\text{pw})}(\mathbf{r}) = \int d\mathbf{r} \langle n_f j_f m_f | (\hat{\mathbf{p}} \cdot \mathbf{e}_{k\Lambda}) e^{i\mathbf{k} \cdot \mathbf{r}} | n_i j_i m_i; k \Lambda \rangle. \quad (11)$$

To express the plane-wave photoabsorption amplitude in terms of Eqs. (8) and (9) we use the known expansion:

$$\mathbf{e}_{k\Lambda} e^{i\mathbf{k} \cdot \mathbf{r}} = \sqrt{4\pi} \sum_{j=1}^{\infty} \sum_{\ell=j-1}^{j+1} i^\ell \sqrt{2\ell+1} j_\ell(kr) C_{\ell 0 1 \Lambda}^{j \Lambda} \mathbf{Y}_{j, \ell, \Lambda}(\Omega). \quad (12)$$

After writing out the sum over the projections ℓ of the TAM of the system and using the following Clebsch–Gordan

coefficients:

$$C_{j-1, 0, 1, \Lambda}^{j, \Lambda} = \sqrt{\frac{j+1}{2(2j-1)}},$$

$$C_{j+1, 0, 1, \Lambda}^{j, \Lambda} = \sqrt{\frac{j}{2(2j+3)}},$$

$$C_{j, 0, 1, \Lambda}^{j, \Lambda} = -\frac{\Lambda}{\sqrt{2}},$$

one arrives at

$$\mathbf{e}_{k\Lambda} e^{i\mathbf{k} \cdot \mathbf{r}} = -\sqrt{4\pi} \sum_{j=1}^{\infty} \sqrt{\frac{(2j+1)}{2}} i^j \times \{i \mathbf{A}_{jm}^E(k, \mathbf{r}) + \Lambda \mathbf{A}_{jm}^M(k, \mathbf{r})\}. \quad (13)$$

This expansion now can be used in Eq. (11):

$$M_{m_f m_i}^{(\text{pw})}(0) = -\sqrt{4\pi} \sum_{j=1}^{\infty} i^{j+\mu} \sqrt{\frac{(2j+1)}{(2j_f+1)}} \Lambda^{\mu+1} C_{j_i, m_i, j, \Lambda}^{j_f, m_f} M_{j\mu}, \quad (14)$$

such that $\mu = 1$ stands for electric multipolarity, and $\mu = 0$ stands for magnetic multipolarity. Here $M_{j\mu}$ stands for the spherical amplitudes of multipolarity μ and order j . Substituting this transition amplitude into the factorization formulas (5), and (7), we express the photoabsorption amplitude in terms of electric and magnetic multipoles.

IV. PHOTOEXCITATIONS IN HIGHLY CHARGED IONS

According to recent theoretical and experimental studies, Boron-like and Sn-like highly charged ions (HCIs) are among the best candidates for the next generation of atomic clocks. At the same time, spectral lines of HCIs are commonly characterized by mixed multipolarity. In this section we use HCIs to demonstrate distinctive features arising from the OAM transfer from the photon and analyze a possibility of separation of multipoles with OAM light.

The photoexcitation rate Γ and cross section σ can be obtained from the above formulas for the transition matrix elements, cf. Refs. [2,37], as

$$\Gamma_{M_{j\mu}}^{(\text{tw})}(b) = 2\pi \delta(E_f - E_i - \omega) \sum_{m_f m_i} |M_{m_f m_i}^{(\text{tw})}|^2,$$

$$\sigma_{M_{j\mu}}^{(\text{tw})}(b) = \Gamma_{M_{j\mu}}^{(\text{tw})}(b) / f(\mathbf{b}). \quad (15)$$

where $f(\mathbf{b})$ is the local (\mathbf{b} -dependent) flux, as in Eq. (4) for Bessel modes.

Analyzing Eq. (5) or (7), one can see that the cross section in the case of an arbitrary transition driven by BB is

$$\sigma_{M_{j\mu}}^{(\text{tw})}(\mathbf{b}) = 2\pi \delta(E_f - E_i - \omega) \frac{A^2}{f(\mathbf{b})} \times \sum_{m_f m_i} \sum_{m'_f m'_i} |J_{m_f - m_y - m_i}(\kappa b) d_{m'_f m'_i}^{j_f} d_{m_i m'_i}^{j_i} \times C_{j j_f j_i} M_{j\mu}|^2, \quad (16)$$

where $C_{jj_f j_i}$ is the coefficient in Eq. (14):

$$C_{jj_f j_i} = -\sqrt{4\pi} i^{j+\mu} \sqrt{\frac{(2j+1)}{(2j_f+1)}} \Lambda^{\mu+1} C_{j_i, m_i, j, \Lambda}^{j_f, m_f}. \quad (17)$$

We start from the low-level transitions with definite multipolarity and initial atomic TAM $j_i = 0$. One can verify that a distinctive feature of the twisted light photoabsorption is that it relaxes the plane-wave selection rules: instead of having only one allowed amplitude for $\Delta m = m_f - m_i \Lambda$, we get $2\Delta j + 1$ amplitudes possible per process, where $\delta_j = j_f - j_i$. The photoabsorption cross section for BB (16) takes the form (cf. Refs. [3,4] that neglected electron's spin):

$$\sigma_{M_{j\mu}}^{(tw)}(\mathbf{b}) = 2\pi\delta(E_f - E_i - \omega) \frac{A^2}{f(\mathbf{b})} \times \sum_{m_f} |C_{00j_f\Lambda}^{j_f m_f} J_{m_f - m_\gamma}(\kappa b) d_{m_f\Lambda}^{j_f}(\theta_k) M_{j_f\mu}|^2, \quad (18)$$

which, for the case of $j_f = 1$, can be shown to be proportional to incoming photon flux $\sigma_{m_f}(\mathbf{b}) \propto |M_{10}^{(pw)}|^2$. Clebsch–Gordan coefficients are coming from coupling of the electromagnetic-field topological charge and helicity to the internal degrees of freedom of the HCl. The multipolarity is determined by the TAM exchange Δj and the parity of the final state. This leads to the conclusion that $E1$ and $M1$ transition rates with the twisted photons are factorizable and proportional to the intensity of the incoming radiation. For the case of multipoles of higher Δj , the characteristic factorization is also present, but the excitation rates acquire extra terms, proportional to $J_{m_\gamma \pm c}^2(\kappa b)$, where $1 < c \leq \Delta j$.

As an example, let us consider transitions from the ground level in Sn-like Pr^{9+} : (1) 351 nm $M1$ transition $^3P_0 \rightarrow ^3P_1$; (2) 426 nm $E2$ transition $^3P_0 \rightarrow ^3F_2$. Corresponding amplitudes for the twisted photons for both $M1$ and $E2$ transitions are shown in Fig. 1 for the BB profile. The use of the BG profile suppresses the amplitudes at the beam periphery depending on the choice of the waist parameter. The rate of $M1$ transition $\Gamma_{M1}^{(tw)} = f\sigma_{M1}^{(tw)}(\mathbf{b})$ appears to be proportional to the electromagnetic flux at the given impact parameter b , making the cross section independent of the atom's position. However, the electric-quadrupole cross section shows the characteristic periodic pattern of peaks dependent on the impact parameter of the system and the pitch angle θ_k . Formally, the cross section for the $E2$ transition becomes singular in the optical vortex center, a phenomenon that can be related to “excitation in the dark” demonstrated experimentally in Refs. [6]; see also Ref. [4] for a discussion of the theory. The photoexcitation cross section for the $E2$ transition as a function of impact parameter b is illustrated in Fig. 2.

Next, we considered transitions with mixed multipolarity, such as $^2P_{1/2} \rightarrow ^2D_{3/2}$ (142 nm) in Boron-like atoms, where the overall local transition amplitude comes from both $E2$ - and $M1$ -type contributions, while $E1$ transitions are parity forbidden. It was calculated by Rynkun *et al.* [38] that the magnetic-dipole contribution is slightly larger than that of the electric-quadrupole contribution in these transitions, $M1/E2 \approx 1.1$. This makes it especially convenient for studying the effects coming from photon topology in mixed-multipolarity states. For the plane-wave case we get two allowed transitions, where

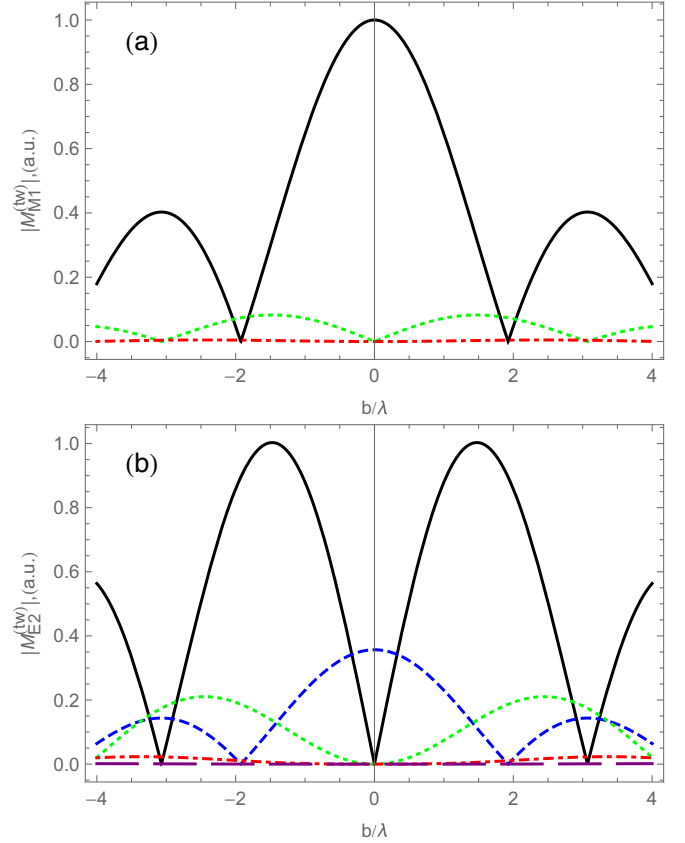


FIG. 1. Dependence of photoabsorption amplitudes of (a) $M1$ ($\lambda = 351$ nm) for $m_\gamma = 1$, and (b) $E2$ ($\lambda = 426$ nm) for $m_\gamma = 2$ transitions in Pr^{9+} HCl of OAM photons with Bessel profile for $\Delta m = 2$ (dashed blue curve), $\Delta m = 1$ (black solid curve), $\Delta m = 0$ (dotted green curve), $\Delta m = -1$ (dot-dashed red curve), $\Delta m = -2$ (long-dashed purple curve). $\Lambda = 1$ (RCP) in both plots.

relative normalization of the multipoles follows from Eq. (16):

$$M_{3/2,1/2}^{(pw)}(0) = i\sqrt{\pi}(E2 - \sqrt{3}M1), \\ M_{1/2,-1/2}^{(pw)}(0) = -i\sqrt{\pi}(\sqrt{3}E2 + M1). \quad (19)$$

For the twisted photons, one can check that the plane-wave amplitudes do not factorize out in this case. However, the whole expression for the OAM cross section remains free of the interference terms. This allows us to use the following equation for the local photoabsorption cross section:

$$\sigma_{M_{j\mu}}^{(tw)}(\mathbf{b}) = 2\pi\delta(E_f - E_i - \omega) \frac{A^2}{f(\mathbf{b})} \times \sum_{m_f m_i} \sum_{m'_f m'_i} |J_{m_f - m_\gamma - m_i}(\kappa b) d_{m_f m'_f}^{3/2} d_{m_i m'_i}^{1/2}|^2 \times C_{j3/2,1/2}^2 |M_{j\mu}|^2, \quad (20)$$

where $M_{j\mu}$ are the multipoles from Eq. (19).

Treating the θ_k as a small parameter $\theta_k \rightarrow 0$, one can expand the expression (16) with local flux $f(\mathbf{b})$, Eq. (4), and get the

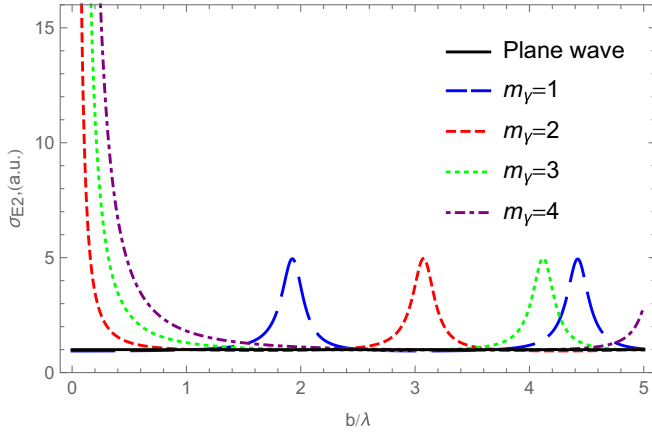


FIG. 2. Photoabsorption cross section for $E2$ in Pr^{9+} HCI by twisted photons with Bessel profile for pitch angle $\theta_k = 0.2$, $\Lambda = 1$ (RCP) and different TAM projections m_γ . The black solid line is the plane-wave cross section normalized to unity; see Ref. [13] for actual lifetimes.

leading terms of the expansion as

$$\sigma_{m_\gamma=1}^{(\text{tw})} \rightarrow 4\pi(E2^2 + M1^2) + O(\theta_k^2), \quad (21)$$

$$\sigma_{m_\gamma=2}^{(\text{tw})} \rightarrow \left(4\pi(E2^2 + M1^2) + \frac{4E2^2}{(b/\lambda)^2\pi} \right) + O(\theta_k^2), \quad (22)$$

$$\sigma_{m_\gamma=3}^{(\text{tw})} \rightarrow \left(4\pi(E2^2 + M1^2) + \frac{16E2^2}{(b/\lambda)^2\pi} \right) + O(\theta_k^2), \quad (23)$$

$$\sigma^{(\text{pw})} = 4\pi(E2^2 + M1^2), \quad (24)$$

where the leading multipole contribution $4\pi(E2^2 + M1^2)$ corresponds to the plane-wave cross section $\sigma^{(\text{pw})}$. Due to the factorization property of BG amplitudes, the derived expression for cross sections apply both for BB and BG modes.

In Fig. 3 the photoexcitation rates for these transitions is plotted as a function of the impact parameter b , where the individual contributions from $E2$ and $M1$ transitions, and their total, are shown for BB profile. Comparing results for two different values of the pitch angle θ_k we find that the rate is smaller for smaller θ_k , which can be understood as the effect of Wigner functions in Eqs. (16), and (20). The use of BG profile suppresses the rate on beam periphery but does not affect relative contributions of $M1$ and $E2$ multipoles. One can see the strong domination of the electric quadrupole over the magnetic dipole in the center of the beam. The effect becomes noticeable for the distances $b \leq \lambda/3$, which for the considered case of $\lambda = 142$ nm is about 50 nm. It imposes position-resolution requirements on the possible experimental observation of the predicted effect.

V. SUMMARY AND OUTLOOK

In this paper we present a theoretical description of the multipolar structure of the twisted light based on the fundamental representation of the photon in its TAM basis. The atomic photoexcitation amplitude is obtained in the form of the multipole expansion.

We analyzed the photoabsorption cross sections of mixed $E2$ - $M1$ transitions in ionized atoms interacting with OAM

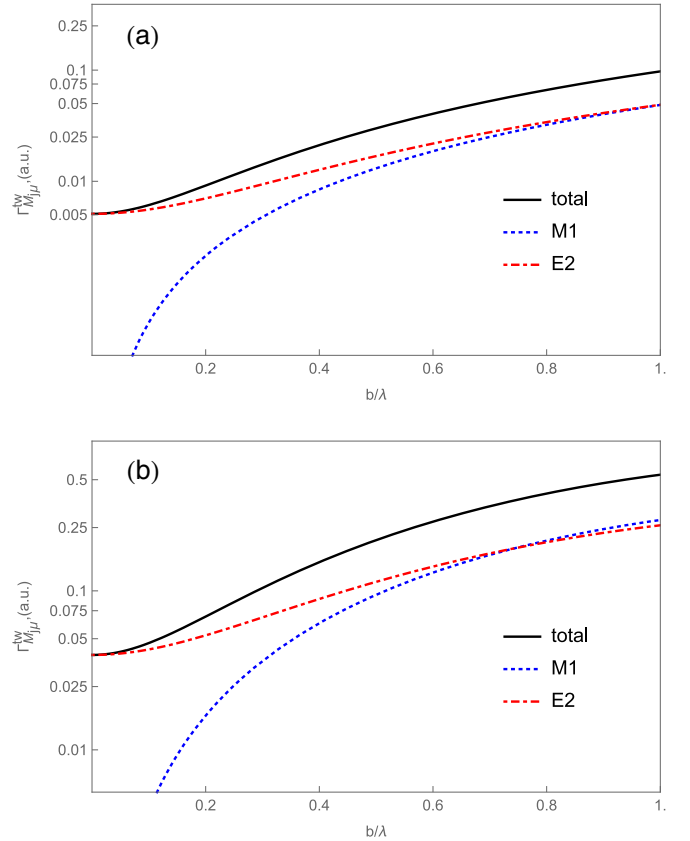


FIG. 3. Log plots of photoabsorption rates in Boron-like HCI for pitch angles (a) $\theta_k = 0.1$ and (b) 0.2. The transitions are excited by twisted photons with Bessel profile, $m_\gamma = 2$, and right-handed helicity ($\Lambda = 1$).

photons, which revealed fundamental differences coming from the photon topology. Two distinct features of the twisted-photon photoexcitation are observed: (a) The magnetic levels population is strongly affected by the topological charge of the photons and (b) the relative contributions of the $M1$ and $E2$ amplitudes into the mixed-multipole transitions depend on the atom's location with respect to the optical vortex axis. According to our theoretical analysis, it is possible to extract the relative transition rates of different multipolar contributions by measuring the photoexcitation rate as a function of the atom's position (or the impact parameter) with respect to the optical vortex center. In this case, only the $E2$ transition survives at the vortex center for the incoming photons carrying two units of angular momentum along the propagation direction. On the other hand, the rates at the beam's periphery are driven by the same relative contribution of multipoles as in the plane-wave case. The proposed method of multipole separation with twisted light requires high position resolution of the target atom's position that can be provided, for example, by Paul traps, as in the recent experiments with $^{40}\text{Ca}^+$ ions [6,7].

In addition, experimental implementation of the proposed technique for HCI would require a source of the twisted light in UV range. Presently, generation of the twisted light up to the extreme UV range (with 99 eV photons) was demonstrated at the synchrotron light source BESSY II [39] and is feasible with new-generation light sources.

ACKNOWLEDGMENTS

The work of A.A. and M.S. was supported in part by the Gus Weiss Endowment of George Washington University. C.E.C. thanks the National Science Foundation for support

under Grant No. PHY-1516509 and thanks the Johannes Gutenberg-University, Mainz, for hospitality as this work was being completed. The authors would like to thank Ferdinand Schmidt-Kaler, Christian Schmiegelow, and Valery Serbo for useful discussions.

-
- [1] L. Allen, M. W. Beijersbergen, R. J. C. Spreeuw, and J. P. Woerdman, *Phys. Rev. A* **45**, 8185 (1992).
 - [2] A. Afanasev, C. E. Carlson, and A. Mukherjee, *Phys. Rev. A* **88**, 033841 (2013).
 - [3] H. M. Scholz-Marggraf, S. Fritzsche, V. G. Serbo, A. Afanasev, and A. Surzhykov, *Phys. Rev. A* **90**, 013425 (2014).
 - [4] A. Afanasev, C. E. Carlson, and A. Mukherjee, *J. Opt.* **18**, 074013 (2016).
 - [5] A. A. Peshkov, D. Seipt, A. Surzhykov, and S. Fritzsche, *Phys. Rev. A* **96**, 023407 (2017).
 - [6] C. T. Schmiegelow, J. Schulz, H. Kaufmann, T. Ruster, U. G. Poschinger, and F. Schmidt-Kaler, *Nat. Commun.* **7**, 12998 (2016).
 - [7] A. Afanasev, C. E. Carlson, C. T. Schmiegelow, J. Schulz, F. Schmidt-Kaler, and M. Solyanik, *New J. Phys.* **20**, 023032 (2018).
 - [8] V. V. Klimov, D. Bloch, M. Ducloy, and J. R. Rios Leite, *Phys. Rev. A* **85**, 053834 (2012).
 - [9] C. Schmiegelow and F. Schmidt-Kaler, *Eur. Phys. J. D* **66**, 157 (2012).
 - [10] S. Franke-Arnold, *Philos. Trans. R. Soc. A* **375**, 20150435 (2017).
 - [11] T. Northup and R. Blatt, *Nat. Photonics* **8**, 356 (2014).
 - [12] T. Ruster, H. Kaufmann, M. Luda, V. Kaushal, C. Schmiegelow, F. Schmidt-Kaler, and U. G. Poschinger, *Phys. Rev. X* **7**, 031050 (2017).
 - [13] M. S. Safronova, V. A. Dzuba, V. V. Flambaum, U. I. Safronova, S. G. Porsev, and M. G. Kozlov, *Phys. Rev. Lett.* **113**, 030801 (2014).
 - [14] J. C. Berengut, V. A. Dzuba, and V. V. Flambaum, *Phys. Rev. Lett.* **105**, 120801 (2010).
 - [15] R. Smitt, L. Å. Svensson, and M. Outred, *Phys. Scr.* **13**, 293 (1976).
 - [16] A. D. Ludlow, M. M. Boyd, J. Ye, E. Peik, and P. O. Schmidt, *Rev. Mod. Phys.* **87**, 637 (2015).
 - [17] E. Träbert, A. Calamai, G. Gwinner, E. Knystautas, E. Pinnington, and A. Wolf, *J. Phys. B: At., Mol. Opt. Phys.* **36**, 1129 (2003).
 - [18] P. Beiersdorfer, *Phys. Scr.* **2009**, 014010 (2009).
 - [19] A. Windberger, J. C. López-Urrutia, H. Bekker, N. Oreshkina, J. Berengut, V. Bock, A. Borschevsky, V. Dzuba, E. Eliav, Z. Harman *et al.*, *Phys. Rev. Lett.* **114**, 150801 (2015).
 - [20] U. I. Safronova, M. S. Safronova, and W. R. Johnson, *Phys. Rev. A* **95**, 042507 (2017).
 - [21] S. Mrozowski, *Rev. Mod. Phys.* **16**, 153 (1944).
 - [22] J. Kwela, A. Kowalski, and J. Heldt, *J. Opt. Soc. Am.* **72**, 1550 (1982).
 - [23] L. Augustyniak, J. Heldt, and J. Bronowski, *Phys. Scr.* **12**, 157 (1975).
 - [24] S. Werbowy and J. Kwela, *J. Phys. B: At., Mol. Opt. Phys.* **42**, 065002 (2009).
 - [25] T. Wařowicz, *Phys. Scr.* **76**, 294 (2007).
 - [26] S. Van Enk and G. Nienhuis, *Europhys. Lett.* **25**, 497 (1994).
 - [27] J. Durnin, J. J. Miceli Jr., and J. H. Eberly, *Phys. Rev. Lett.* **58**, 1499 (1987).
 - [28] M. Born and E. Wolf, *Principles of Optics: Electromagnetic Theory of Propagation, Interference and Diffraction of Light* (Cambridge University Press, Cambridge, 2013).
 - [29] U. D. Jentschura and V. G. Serbo, *Phys. Rev. Lett.* **106**, 013001 (2011).
 - [30] K. Y. Bliokh, M. A. Alonso, E. A. Ostrovskaya, and A. Aiello, *Phys. Rev. A* **82**, 063825 (2010).
 - [31] K. Y. Bliokh, E. A. Ostrovskaya, M. A. Alonso, O. G. Rodríguez-Herrera, D. Lara, and C. Dainty, *Opt. Express* **19**, 26132 (2011).
 - [32] L. Kaplan and J. H. McGuire, *Phys. Rev. A* **92**, 032702 (2015).
 - [33] C. Sheppard and T. Wilson, *IEEE J. Microwaves, Opt. Acoust.* **2**, 105 (1978).
 - [34] A. Kiselev, *Opt. Spectrosc.* **96**, 479 (2004).
 - [35] D. L. Andrews and M. Babiker, *The Angular Momentum of Light* (Cambridge University Press, Cambridge, 2012).
 - [36] A. Akhiezer and V. Berestetskii, *Quantum Electrodynamics, 1965* (Interscience, New York, 1959).
 - [37] A. Afanasev, C. E. Carlson, and M. Solyanik, *J. Opt.* **19**, 105401 (2017).
 - [38] P. Rynkun, P. Jönsson, G. Gaigalas, and C. F. Fischer, *At. Data Nucl. Data Tables* **98**, 481 (2012).
 - [39] J. Bahrtdt, K. Holldack, P. Kuske, R. Müller, M. Scheer, and P. Schmid, *Phys. Rev. Lett.* **111**, 034801 (2013).